

I-V and Gain Characteristics of Electrowetting-Based Liquid Field Effect Transistor

Duk Young Kim, Stephen Herman, and Andrew J. Steckl¹

Nanoelectronics Laboratory, University of Cincinnati, Cincinnati, Ohio 45221-0030, USA

Keywords: electrowetting, microfluidics, hydrophobic surface, electrolyte, field effect transistor (FET)

There is great interest in μ fluidic devices due to important applications ranging from biotechnology [1] to flat panel displays [2]. An important enabling technology in μ fluidics is based on the electrowetting (EW) effect [3], which controls the contact angle of a liquid on a hydrophobic surface through the application of an electric field. Many operations can be performed through external control [4] (such as droplet dispensing, transport, splitting, and mixing), leading to increasingly sophisticated applications for *lab-on-chip* [5] devices. One of the limitations of μ fluidic devices is that the information contained in the fluid has to be converted in an electronic form in order to interact with our pervasive digital world. This conversion typically is performed through either direct optical sensing or combined with optical excitation of fluorescent dyes, which is cumbersome, limited in information processing, and expensive. We have invented [6] an EW-based liquid state field effect transistor (LiquiFET), which is very similar in concept to conventional semiconductor FETs but operates in the liquid state and thus can directly convert charge-related information from the liquid state into conventional electronic signals. Fig. 1 illustrates the LiquiFET structure and current control achieved by EW between competitive conducting/insulating fluids.

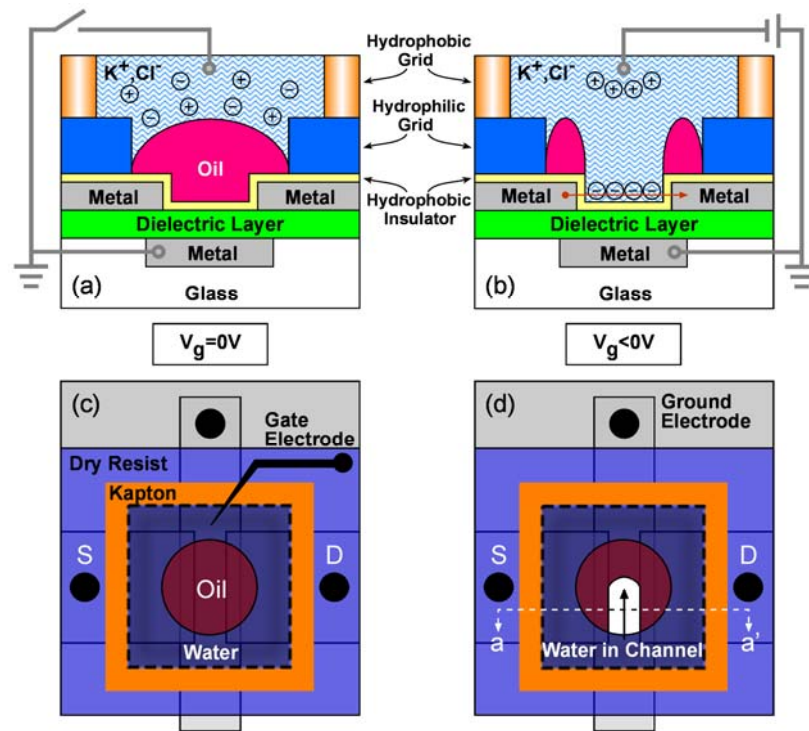


Fig. 1 Schematics of LiquiFET structure: (a) cross section in off state, (b) cross section in on state, (c) top view in off state, and (d) top view in on state.

¹ a.steckl@uc.edu

The device structure consists of the glass substrate, an Al₂O₃-covered transparent ground electrode (ITO), source and drain metal contacts (ITO), a hydrophobic insulator (amorphous fluoropolymer), a hydrophobic/hydrophilic grid (Kapton/SU-8), the two fluids (electrolyte/oil), and the top gate electrode (Au wire). We used electrolyte as the conducting medium and an oil film for the electrical switching. Figs. 1(a) and 1(b) show cross-section (a-a' section) schematics of the LiquiFET under OFF (zero gate bias) and ON (negative gate bias) conditions, respectively. For zero gate bias, the oil preferentially covers the hydrophobic insulator, forming a thin film that excludes the electrolyte solution (Fig. 1(c)). When negative bias is applied to the gate, the resulting field attracts the water molecules and electrolyte anions to the hydrophobic insulator surface. The water displaces the oil layer and forces the displaced oil to the side regions of the structure, as shown in Figs. 1(b) and 1(d). In the process, the presence of the electrolyte in the channel region enables current conduction between source and drain. Fig. 2 shows displacement of the oil droplet in the channel region of actual devices with 400 μm and 100 μm channel length, respectively. At zero bias (Figs. 2(a) and 2(d)), the oil layer covers the entire hydrophobic surface in the channel region, and the transistor is in the electrically off state. As the gate bias is increased, EW forces a conducting channel to be formed, establishing the LiquiFET drain current (Figs. 2(b) and 2(e)). At a slightly higher voltage (Figs. 2(c) and 2(f)), the channel is completely open. Figs. 3 and 4 show I-V characteristics and transconductance of LiquiFET with different gate biases for 100 and 400 μm channels. The shorter channel LiquiFET results in higher current and transconductance, which is also one of the basic characteristics of conventional semiconductor FETs. For a 100 μm channel LiquiFET, the measured transconductance is 70 nS at $V_{\text{DS}} = 4\text{V}$, which is about 3.5 times higher than that of a 400 μm channel LiquiFET. Typical device turn-on voltage is in the range of 2.5 – 3V and the on/off current ratio is over 10,000. In parallel with the experimental investigation, we are carrying out modeling and simulation of the LiquiFET operation. The approach being explored is to use conventional FET model in conjunction with charge transport in conducting liquids.

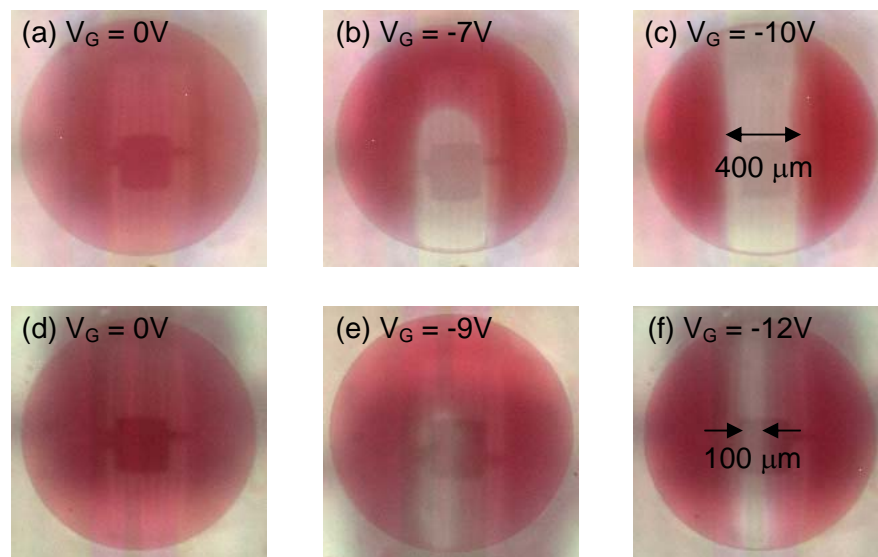


Fig. 2 Photographs of LiquiFET showing the effect of gate bias: (a) 0, (b) -7, and (c) -10 V for 400 μm channel, (d) 0, (e) -9, and (f) -12 V for 100 μm channel. Oil contains red dye for visualization purpose.

Fig. 5 shows a preliminary simulation result indicating the electric field distribution in the LiquiFET, which is similar to the conventional FET model. Our previous report [6] has determined that the channel mobility, μ_N , of the LiquiFET is $\sim 1 \text{ cm}^2/\text{Vsec}$. Using the diffusivity [7] of KCl, we calculated the ionic mobility of anions in the channel from the Einstein's equation. With $D_N = 1.9 \times 10^{-5} \text{ cm}^2/\text{sec}$, the calculated μ_N is $7.46 \times 10^{-4} \text{ cm}^2/\text{Vsec}$ and much less than the measured channel mobility. This means that the carrier transport and current flow in the LiquiFET is not due to ionic transport, but rather electronic transport and other mechanisms such as field-assisted hopping and tunneling.

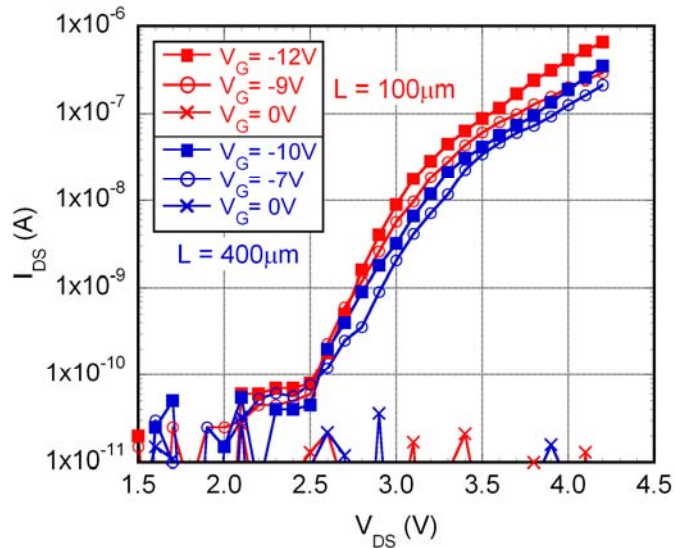


Fig. 3 I-V characteristics of LiquiFET: drain current vs. drain voltage for 400 μm and 100 μm channel at different gate biases.

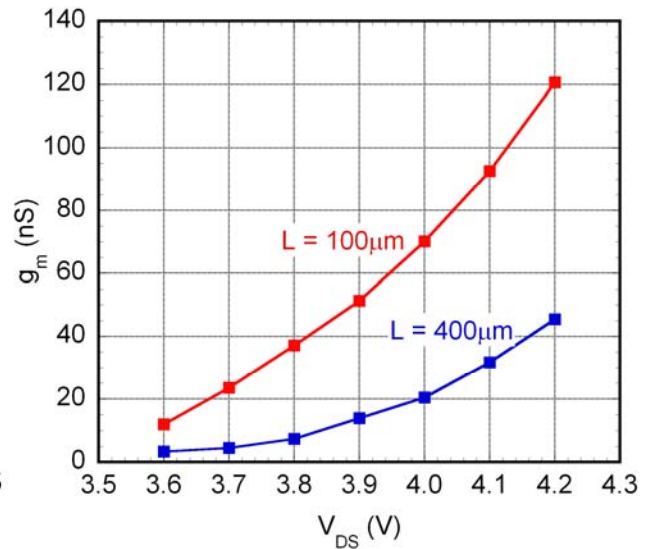


Fig. 4 Measured transconductance of LiquiFET for 400 μm and 100 μm channel.

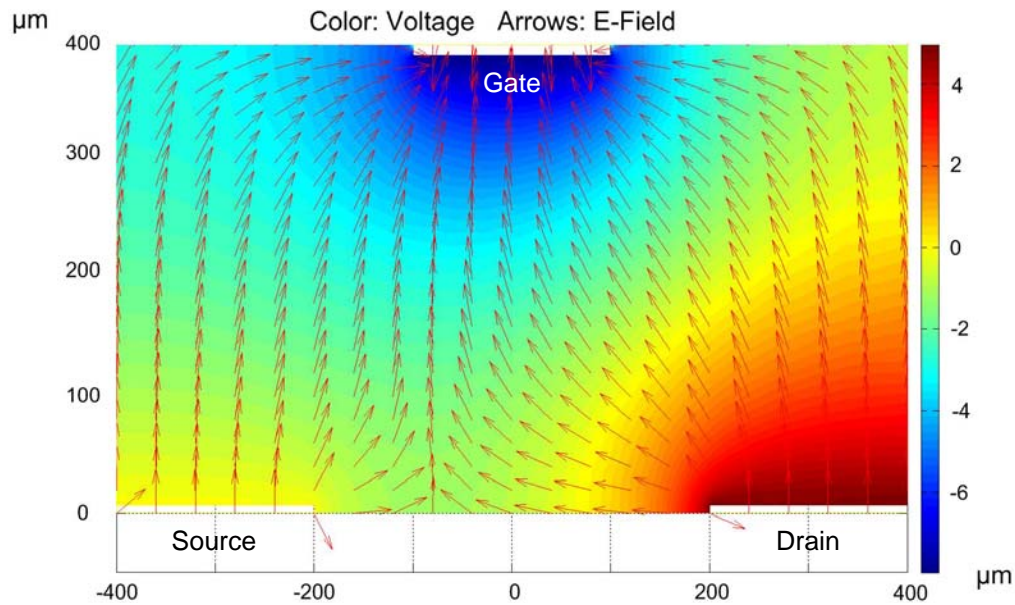


Fig. 5 Simulation of electrostatic field distribution inside the LiquiFET at $V_{GS} = -8\text{V}$ and $V_{DS} = 5\text{V}$. Color scale is in volts and vector arrows indicate the direction of electric field.

References

- [1] V. Srinivasan, V. K. Pamula, and R. B. Fair, "An integrated digital microfluidic lab-on-a-chip for clinical diagnostics on human physiological fluids," *Lab on a Chip*, vol. 4, pp. 310-315, 2004.
- [2] J. C. Heikenfeld and A. J. Steckl, "Liquid Light," *Information Display*, pp. 26-31, Nov. 2004 2004.
- [3] T. B. Jones, "An electromechanical interpretation of electrowetting," *Journal of Micromechanics and Microengineering*, vol. 15, pp. 1184-1187, 2005.
- [4] S. K. Cho, H. Moon, and C.-J. Kim, "Creating, transporting, cutting, and merging liquid droplets by electrowetting-based actuation for digital microfluidic circuits," *Journal of Microelectromechanical Systems*, vol. 12, pp. 70-80, 2003.
- [5] J. Y. Yoon and R. L. Garrell, "Preventing Biomolecular Adsorption in Electrowetting-Based Biofluidic Chips," *Analytical Chemistry*, vol. 75, pp. 5097-5102, 2003.
- [6] D. Y. Kim and A. J. Steckl, "Liquid-state field-effect transistors using electrowetting," *Applied Physics Letters*, vol. 90, pp. 043507-3, 2007.
- [7] H. S. Harned, "The diffusion coefficients of the alkali metal chlorides and potassium and silver nitrates in dilute aqueous solutions at 25C," *Proceedings of the National Academy of Sciences*, vol. 40, pp. 551-556, 1954.